



Published in final edited form as:

Toxicol Lett. 2010 March 1; 193(1): 94. doi:10.1016/j.toxlet.2009.12.012.

The Role of NOX Enzymes in Ethanol-induced Oxidative Stress and Apoptosis in Mouse Embryos

Jian Dong^a, Kathleen K Sulik^a, and Shao-yu Chen^b

^a Bowles Center for Alcohol Studies and Department of Cell and Developmental Biology, University of North Carolina at Chapel Hill, Chapel Hill, NC 27599-7178

^b Department of Cancer Biology and Pharmacology, University of Illinois College of Medicine at Peoria, Peoria, IL 61605-2576

Abstract

Reactive oxygen species (ROS) play an important role in ethanol-induced apoptosis and teratogenesis. However, the major sources of ROS in ethanol-exposed embryos have remained undefined. This study was conducted to determine the role of NADPH oxidase (NOX) in ethanol-induced oxidative stress and apoptosis in mouse embryos. Analyses of mRNA expression indicated that ethanol treatment resulted in a significant increase in mRNA expression of NOX catalytic subunit Duox-1 in gestational day 9 (GD 9:0) mouse embryos. Ethanol exposure also resulted in significant increases in mRNA expression of NOX regulatory subunits, p22phox, p67phox, NOXA1 and NOXO1. In addition, a significant increase in NOX enzyme activity was found in the ethanol-exposed embryos as compared to controls. Co-treatment with the NOX inhibitor, diphenyleneiodonium (DPI), significantly prevented ethanol-induced increases in NOX enzyme activity, ROS generation and oxidative DNA damage in ethanol-exposed embryos. DPI treatment also resulted in a reduction in caspase-3 activation, decreased caspase-3 activity and diminished prevalence of apoptosis in ethanol-exposed embryos. These results support the hypothesis that NOX is a critical source of ROS in ethanol-exposed embryos and that it plays an important role in ethanol-induced oxidative stress and pathogenesis.

Keywords

NADPH oxidase; Fetal Alcohol Spectrum Disorder; reactive oxygen species; embryo; apoptosis

1. Introduction

Prenatal ethanol exposure results in a range of abnormalities that is now termed the Fetal Alcohol Spectrum Disorder (FASD). This spectrum of birth defects includes abnormalities in a number of organ systems, with those involving the brain being very prevalent (Roebuck et al., 1998). Indeed, prenatal ethanol exposure is now recognized as the leading known non-genetic cause of mental retardation in the Western world (Abel and Sokol, 1986).

Author to whom correspondence should be sent: Shao-yu Chen, Ph.D., Department of Cancer Biology and Pharmacology, University of Illinois College of Medicine at Peoria, Peoria, IL 61605-2576, Phone: (309) 671-8538, FAX: (309) 671-8403, sychen@uic.edu.

Conflict of interest statement: The authors declare that there are no conflicts of interest.

Publisher's Disclaimer: This is a PDF file of an unedited manuscript that has been accepted for publication. As a service to our customers we are providing this early version of the manuscript. The manuscript will undergo copyediting, typesetting, and review of the resulting proof before it is published in its final citable form. Please note that during the production process errors may be discovered which could affect the content, and all legal disclaimers that apply to the journal pertain.

In both *in vivo* and *in vitro* FASD model systems, cell death in selected cell populations is a commonly observed pathologic feature (Bonthius et al., 2006; Chen et al., 2001; Dunty, Jr. et al., 2001). For example, Kotch and Sulik (Kotch and Sulik, 1992) as well as Dunty et al. (Dunty, Jr. et al., 2001) noted excessive cell death that was located in specific regions of the brain of gestational day 8.5 to 9 (GD 8.5 to 9; equivalent to the fourth week of human gestation) ethanol-exposed mouse embryos. In addition, ethanol exposure during the period of brain development that is comparable to that of the human third trimester causes death of postmitotic neurons in the hypothalamus (De et al., 1994), cerebral cortex (Olney et al., 2002), cerebellum (Tran et al., 2005), and associated brain-stem structures (Napper and West, 1995). Using TUNEL staining, the ethanol-induced cell death in early embryos has been shown to be apoptotic (Chen et al., 2001; Chen et al., 2004; Dunty, Jr. et al., 2001).

There is growing evidence that oxidative stress plays an important role in ethanol-induced apoptosis and teratogenesis (Henderson et al., 1999; Wentzel et al., 2006). Prenatal ethanol exposure results in oxidative stress in neural crest cells (Chen and Sulik, 1996; Chen and Sulik, 2000; Davis et al., 1990), cultured cortical neurons (Ramachandran et al., 2003), and cerebellar tissue (Heaton et al., 2006). These results are supported by studies that have shown that 1) superoxide dismutase (SOD) can diminish ethanol-induced superoxide anion generation, lipid peroxidation and cell death in cultured mouse embryos, and can significantly reduce the incidence of neural tube defects (Kotch et al., 1995); 2) EUK-134, a synthetic SOD and catalase mimetic can prevent apoptosis and the resulting limb defects in mouse embryos exposed to ethanol *in vivo* (Chen et al., 2004) and 3) transcriptional induction of endogenous antioxidants through Nrf-2 activation can prevent ethanol-induced oxidative stress and apoptosis in mouse embryos (Dong et al., 2008).

Although many pathways have been suggested to contribute to the ability of ethanol to induce a state of oxidative stress, the major sources of reactive oxygen species (ROS) in ethanol-exposed embryos have not been defined. Potential sources of ROS in the cells include mitochondrial respiratory chain enzymes, xanthine oxidase, cytochrome P450 enzymes (e.g. CYP2E1) (Halliwell, 1991; Wu and Cederbaum, 2003) and NADPH oxidase (NOX). The latter has only very recently begun to receive considerable research attention (Sumimoto, 2008).

NOX enzymes were initially discovered in phagocytic cells. They are composed of multiple subunits, including a glycoprotein gp91phox, which is considered to be directly involved in the generation of superoxide anion (Bedard and Krause, 2007). Homologues of gp91phox, including NOX1 through NOX5, and the dual oxidases Duox1 and Duox2, have recently been described in non-phagocytic cells (Lambeth, 2004). Activation of NOX enzymes involves cytoplasmic components, including p47phox, p67phox, NOXO1 and NOXA1, as well as small GTPase RAC (RAC2 and/or RAC1) (Lambeth, 2004). NOX enzymes can catalyze NADPH-dependent reduction of oxygen to generate superoxide anion (Babior, 2002). Recently, NOX enzymes have emerged as a major source of ROS in neurons, glia, and cerebral blood vessels (Gao et al., 2003; Infanger et al., 2006; Miller et al., 2006). NOX-mediated apoptosis has also been observed in human aortic smooth muscle cells exposed to 7-ketocholesterol (Pedruzzi et al., 2004), and in angiotensin II-exposed H9C2 cardiac muscle cells (Qin et al., 2006). It is also noteworthy that two NOX inhibitors, diphenyleneiodonium (DPI) and apocynin, can diminish superoxide generation and liver injury in hemorrhagic shock (Abdelrahman et al., 2005). DPI is a well-characterized and potent NOX inhibitor. Studies have shown that DPI can abstract an electron from FAD to form a radical, which then forms covalent adducts binding irreversibly to the FAD of NOX enzymes, thus blocking their activity (O'Donnell et al., 1993).

This study was designed to define the role of NOX enzymes in ethanol-induced oxidative stress and apoptosis in mouse embryos. To this end, mRNA expression of NOX catalytic and regulatory subunits was analyzed using quantitative real-time PCR. In addition, the potential

of the NOX enzyme inhibitor, DPI, to prevent ethanol-induced oxidative stress and apoptosis in mouse embryos was examined. The results of this study support the hypothesis that NOX is a critical source of ROS in ethanol-exposed mouse embryos and that inhibition of NOX can prevent ethanol-induced oxidative stress and apoptosis. These results provide important clues for intervention strategies that may aid in diminishing the incidence and/or severity of FASD.

2. Materials and methods

2.1. Animal care and dosing

C57BL/6J mice (The Jackson Laboratory, Bar Harbor, ME) were mated for 2 hours early in the light cycle. The time of vaginal plug detection was considered 0 days, 0 h of gestation (GD 0:0). Mice were maintained on an *ad libitum* diet of breeder chow and water. Pregnant mice in the experimental groups were administered two intraperitoneal (ip) doses of 2.9 g/kg ethanol alone or two comparable doses of ethanol in combination with one 4.0 mg/kg dose of DPI (Sigma, St. Louis, MO, USA). The injections were given 4 hours apart, with the DPI and the first dose of ethanol administered on gestational day 9 (GD9:0). Control animals were injected with lactated Ringer's solution according to the above regimen. This treatment regimen produced a peak maternal blood alcohol level (BAL) of approximately 500 mg/dL 4.5 hours after the initial dose. At 6 hours after the first dose, the time at which pregnant mice were killed and the embryos were prepared for analysis of mRNA expression, ROS generation and oxidative DNA damage, the maternal BAL is approximately 400 mg/dL (Webster et al., 1983). Previous studies have shown that at early developmental stages in mice, acute administration of ethanol that yields peak maternal blood alcohol concentrations of 400-500 mg/dL (approximately 85-105 mM) is required to 1) induce excessive apoptosis (Dunty, Jr. et al., 2001; Kotch and Sulik, 1992); 2) induce malformations that are characteristic of FAS (Kotch and Sulik, 1992; Sulik et al., 1981); and 3) induce significant changes in gene and protein expression (Dong et al., 2008; Green et al., 2007). Although the concentration is high, it is not outside of that which can be observed in chronic alcoholics (Adachi et al., 1991). Only this particular dose of ethanol was chosen because the purpose of this study is to determine whether Nox is involved in oxidative stress in mouse embryos exposed to ethanol at a dose that has been demonstrated to be able to induce both apoptosis and FAS-like malformation. For apoptosis analysis, pregnant mice were killed on GD 9:12 (12 hours after the first ethanol treatment). Selection of the time points at which analyses were conducted was based on our previous investigations (Chen et al., 2004; Dong et al., 2008; Dunty, Jr. et al., 2001; Kotch and Sulik, 1992). Embryos were dissected free of their deciduas in lactated Ringer's solution and then staged by counting the number of somite pairs. Embryos of comparable developmental stage were pooled for mRNA and protein preparation. Whole embryos were used for mRNA and protein analysis because very limited tissue can be collected from mouse embryos at this early developmental stage that is highly sensitive to ethanol-induced birth defects. All protocols used in this study were approved by the University of North Carolina at Chapel Hill Institutional Animal Care and Use Committee.

2.2. RNA isolation and reverse-transcription reaction

Total RNA was isolated from whole embryos using Trizol reagent (Invitrogen, Carlsbad, CA, USA) and cleaned with Qiagen RNeasy Mini Kit (Qiagen, Hilden, Germany) according to the manufacturer's instructions. RNA quantitation was performed by measuring the absorbance of the RNA sample solutions at 260 nm. The RNA integrity was determined by agarose gel electrophoresis. The RNA samples were treated with DNase-I (Qiagen RNase-free DNase kit). The reverse transcription reaction was carried out in a 100 μ l reaction by incubation of 1 μ g of RNA with Oligo d (T)16 primers at 48°C for 60 min., using a commercially available GeneAmp RNA PCR kit (Applied Biosystems, USA).

2.3. Quantitative real-time PCR

Quantitative real-time PCR with SYBR green I detection (Applied Biosystems, Warrington, UK) was performed in a MyiQ Single-Color Real-Time PCR Detection System (Bio-Rad, CA, USA). Primers listed in Table 1 were designed using Primer Express Software (Applied Biosystems) and synthesized by Integrated DNA Technologies, Inc (Coralville, IA, USA). Reactions were performed in a total volume of 25 μ l, including 12.5 μ l 2 \times Power SYBR[®] Green PCR Master Mix, 1 μ l of 0.4 μ M primer, and 2.5 μ l of the previously reverse-transcribed cDNA template on a 96-well iCycler iQ PCR plates (Bio-Rad, CA, USA). All reactions were carried out at least in duplicate for each sample. The thermo-cycling profile included 45 cycles consisting of denaturation at 95 $^{\circ}$ C for 15 sec, annealing and elongation at 60 $^{\circ}$ C for 60 sec. Melting curve and agarose electrophoresis analysis were performed to exclude amplification of non-specific products. GAPDH was used as a reference for normalization and relative quantification was performed using iCycler iQ Optical System Software Version 1 (Bio-Rad, CA, USA).

2.4. NOX enzyme activity assay

The activity of NOX enzyme was determined by the method described by Cui and Douglas (Cui and Douglas 1997), with modification. Embryos were washed twice in ice-cold PBS and homogenized in buffer containing 20 mM KH₂PO₄, 1 mM EGTA, 10 μ g/ml aprotinin, 25 μ g/ml leupeptin and 1 mM phenylmethylsulfonyl fluoride. The assay was started by adding homogenate into 50 mM phosphate buffer (pH 7.0) containing 1 mM EGTA, 150 mM sucrose, 500 μ M lucigenin, and 100 μ M NADPH. Photoemission was measured every minute for 14 min using a Luminometer (Wallac 1420 Multilabel Counter, PerkinElmer Life and Analytical Sciences, MA, USA). The protein concentration in each sample was measured using Bio-Rad Protein Assay Reagent (Bio-Rad Laboratories, Inc., Hercules, CA, USA) according to the manufacturer's instructions. NOX enzyme activity was expressed as relative light units (RLU).

2.5. Measurement of ROS generation

ROS generation was assayed as described previously (Dong et al., 2008). Briefly, the mouse embryos were washed twice in assay buffer (130 mM KCl, 5 mM MgCl₂, 20 mM NaH₂PO₄, 20 mM Tris-HCl, 30 mM glucose) then homogenized in 100 μ l of the buffer. The homogenate was centrifuged at 10,000 g for 15 min at 4 $^{\circ}$ C and the supernatant, which was equivalent to 40 μ g of protein, was transferred to a 96-well micro-plate. Assay buffer and 2 μ l of 2',7'-dichlorodihydro-fluorescein diacetate (DCHFDA; Molecular Probes Inc., Eugene, OR, USA) (5 mM in DMSO) were added to the micro-plate to give a total reaction volume of 200 μ l. Subsequently, the samples were incubated at 37 $^{\circ}$ C for 15 min. The fluorescence intensity was monitored for 30 min after excitation at 485 nm and emission at 535 nm using a CytoFluor fluorescence plate reader (Perseptive Biosystems, Foster City, CA, USA). The protein concentration in each sample was measured using Bio-Rad Protein Assay Reagent (Bio-Rad Laboratories, Inc., Hercules, CA, USA) according to the manufacturer's instructions. The ROS level was expressed as relative fluorescence intensity units.

2.6. Measurement of oxidative DNA damage

Oxidative DNA damage was determined by measuring the level of 8-OH deoxyguanosine (8-OHdG), a sensitive index of oxidative DNA damage (Hamilton et al., 2001). DNA from mouse embryos was isolated with a DNeasy Tissue kit (Qiagen, Hilden, Germany) according to the manufacturer's instructions and dissolved in 20 mM sodium acetate buffer (pH 5.2). The isolated DNA was treated with nuclease P1 (Sigma) to digest DNA to nucleotides, followed by incubation with alkaline phosphatase (Fermentas Inc., Hanover, MD, USA) for 1 hour. 100 μ g of DNA was assayed for levels of 8-OHdG using a 8-OHdG-EIA kit (Oxis Health Products, Inc., Portland, OR, USA) according to the manufacturer's instructions.

2.7. Apoptosis assays

Apoptosis was determined in GD 9 mouse embryos 12 hours after initial maternal ethanol exposure using two independent assays, caspase-3 analysis and Nile blue sulfate vital staining. Caspase-3 activation was analyzed by Western blot. For this assay, embryos were washed once in phosphate-buffered saline (PBS), and lysed by incubation for 30 min in RIPA lysis buffer (PBS, 0.5 % Sodium Deoxycholate, 1 % NP-40, 0.1 % SDS, 1 mM Dithiothreitol) with 1 mM PMSF and protease cocktail inhibitors (Roche, USA). The samples were then centrifuged at 16,000 g for 10 min at 4 °C. The collected supernatants were used for Western blotting. The protein concentration in each sample was measured using Bio-Rad Protein Assay Reagent (Bio-Rad Laboratories, Inc., Hercules, CA, USA) according to the manufacturer's instructions. Western blots were performed by standard protocols. Briefly, total protein (20 µg each lane) was resolved on an SDS- 10% polyacrylamide gel and transferred to nitrocellulose membranes. The levels of caspase-3 were analyzed with rabbit polyclonal against cleaved caspase-3 (Asp 175) (1:500, Cell Signaling Technology, Danvers, MA), followed by detection with ECL plus Western blotting detection reagents (GE Healthcare, Piscataway, NJ). The membranes were scanned on a Bio-Rad Versa Doc™ Imaging System (Model 4000) and the intensity of the protein bands was analyzed using Bio-Rad Quantity One software (Version 4.5.1). The extent of apoptosis was expressed as fold change in caspase-3 activation over control. Caspase-3 activity was determined by fluorimetric assay using the substrate Ac-DEVD-AMC (Caspase-3 Cellular Activity Assay Kit, Calbiochem, San Diego, CA) according to the manufacturer's instruction. Nile blue sulfate staining was carried out in whole embryos as described previously (Chen et al. 2001). Briefly, embryos were incubated in a 1:50,000 solution of Nile blue sulfate in Ringer's solution at 37°C for 30 min. Stained specimens were then washed in Ringer's solution and immediately photographed using an Olympus dissecting photomicroscope. Both experimental and control embryos were processed simultaneously for visual comparison of patterns of cell death. Approximately 10 - 15 embryos for both experimental and control groups were examined.

2.8. Statistical analysis

Statistical analyses were performed using StatView software (SAS Institute Inc, Cary, NC). All data are expressed as mean ± SEM of three separate experiments. Statistical comparisons between groups were analyzed by a One-way ANOVA. Multiple comparison post-tests between groups were conducted using a Tukey's test. Differences between control and treated groups, or between ethanol-treated group and other groups were considered significant at $p < 0.05$.

3. Results

3.1. Ethanol exposure significantly increases mRNA expression of NOX catalytic and regulatory subunits as well as NOX activity in mouse embryos

To determine the role of NOX enzymes in ethanol-induced ROS generation, mRNA expression of NOX catalytic and regulatory subunits was analyzed in GD9 mouse embryos following 6 hours of *in vivo* ethanol exposure. While mRNA expression of NOX catalytic subunits NOX1, NOX2, NOX3, NOX4 and Duox2 were not altered by ethanol, a significant increase in mRNA expression of Duox1 was observed (Fig. 1). The ethanol exposure also resulted in significant increases in mRNA expression of NOX regulatory subunits, including p22phox, p67phox, NOX activator 1 (NOXA1), NOX organizer 1 (NOXO1) and a Rho-family small GTPase RAC1 (Fig. 2). In addition, a significant increase in NOX enzyme activity was found in the ethanol-exposed embryos as compared to controls (Fig. 3).

3.2. Inhibition of NOX enzymes with DPI significantly reduces ROS generation and oxidative DNA damage in mouse embryos exposed to ethanol *in vivo*

To further test whether NOX is a major source of ROS in ethanol-exposed mouse embryos, we have used the NOX inhibitor, DPI, to determine whether inhibition of NOX can prevent ethanol-induced ROS generation and oxidative stress in this model system. As shown in Fig. 3, co-treatment with DPI significantly decreased NOX enzyme activity in ethanol-exposed mouse embryos, indicating that this compound can effectively inhibit NOX enzymes. To analyze the effects of DPI treatment on ROS generation, a 2',7'-dichlorodihydro-fluorescein diacetate (DCHFDA) assay was used. Exposure of mouse embryos to ethanol for 6 hours *in vivo* was found to significantly increase ROS generation, providing confirmation that ethanol can induce ROS generation in early mouse embryos. Co-treatment with DPI significantly prevented ethanol-induced increases in ROS generation in the ethanol-exposed mouse embryos (Fig. 4). As indicated by significantly increased 8-OHdG content, ethanol treatment resulted in a significant increase in oxidative DNA damage in the embryos, while co-treatment with DPI significantly prevented ethanol-induced increases in oxidative DNA damage (Fig. 5).

3.3. Co-treatment with DPI results in a significant reduction in caspase-3 activation, decreases caspase-3 activity, and diminishes the prevalence of apoptosis in mouse embryos exposed to ethanol *in vivo*

To determine whether NOX-mediated oxidative stress is a key contributor to ethanol-induced apoptosis in mouse embryos, caspase-3 activation and Nile blue sulfate staining were examined following DPI treatment. As shown in Figure 6. A, little active caspase-3 was observed in control embryos. *In vivo* ethanol treatment induced the activation of caspase-3 in mouse embryos as evidenced by a significant increase in the expression of its 17 kDa subunit. Ethanol exposure also resulted in a significant increase in the activity of this protease (Fig. 6, B). Co-treatment with DPI resulted in a significant reduction in the activation and activity of caspase-3 in ethanol-exposed mouse embryos as compared to the group treated with ethanol alone (Fig. 6). This is consistent with Nile blue sulfate staining results. Compared with the untreated and DPI treated control embryos, those exposed to ethanol showed excessive Nile blue sulfate staining in the first branchial arch, the forebrain and the hindbrain. The pattern and amount of stain uptake in the ethanol-exposed embryos is typical of that previously reported for this exposure paradigm (Dunty, Jr. et al., 2001). Co-treatment with DPI greatly prevented the ethanol-induced increase in Nile blue sulfate staining (Fig. 7), indicating that co-treatment with DPI is, indeed, effective in preventing ethanol-induced apoptosis in this FASD model.

4. Discussion

Although the role of oxidative stress in ethanol-induced apoptosis and subsequent teratogenesis has been evidenced in previous studies (Chen et al., 2004; Davis et al., 1990; Dong et al., 2008; Kotch et al., 1995), the intracellular sources of ROS in ethanol-exposed embryos have remained undefined. The importance of identifying these intracellular sources of ROS lies in the potential to block ethanol-induced ROS generation in early embryos and, ultimately, to prevent birth defects caused by ethanol.

As previously noted, there are a number of potential sources of ROS production in the cells. Among these is xanthine oxidase, which is a well-documented biologic source of superoxide anion and which has been implicated in the pathogenesis of various tissue injuries and disease conditions, including ethanol-induced hepatotoxicity (Harrison, 2002; Wu and Cederbaum, 2003). Cytochrome P450 2E1 (CYP2E1) is another potential source of ROS in ethanol-exposed mouse embryos. It is involved in the metabolism and activation of many toxicological substrates, and can generate ROS during its catalytic cycle (Lu and Cederbaum, 2008), and has received considerable interest in the ethanol research field. Importantly, CYP2E1-

dependent oxidative stress has been shown to contribute to the toxic action of ethanol on the liver (Lu and Cederbaum, 2008). It is also noteworthy that low levels of CYP2E1 are expressed in human fetal liver by 19 weeks of gestation and in human prenatal brain at GD 50 (Brzezinski et al., 1999; Carpenter et al., 1996). In addition, induction of CYP2E1 by ethanol has been observed in GD 20 fetal rat liver (Carpenter et al., 1997). These results have led to the suggestion that CYP2E1-derived ROS may play a role in the pathogenesis of FAS (Brzezinski et al., 1999; Carpenter et al., 1996).

More recently, NOX enzymes have been demonstrated to play an important role in ROS generation (Sumimoto, 2008). Among the seven-member NOX protein family are Duox 1 and 2, which were originally identified in the thyroid gland (Geiszt et al., 2003), and are also expressed in the entire intestinal tract (El Hassani et al., 2005), salivary glands (Geiszt et al., 2003), and airways (Forteza et al., 2005; Geiszt et al., 2003) as well as in human fetal lung epithelial cells (Fischer et al., 2007). Duox produces hydrogen peroxide directly or indirectly by dismutation of superoxide (Forteza et al., 2005; Geiszt et al., 2003). In this study, we have demonstrated that ethanol exposure results in a significant increase in mRNA expression of Duox1 in GD 9 mouse embryos, suggesting that NOX is involved in their ROS generation. In addition, the ethanol treatment significantly increased mRNA expression of the NOX regulatory components, p22phox, p67phox, NOXO1, NOXA1 and RAC1. Ethanol-induced transcriptional up-regulation of NOX regulatory components, which control NOX dependent ROS production, further supports the hypothesis that NOX is involved in the production of ROS in ethanol-exposed mouse embryos.

That the NOX inhibitor, DPI, was shown to decrease NOX enzyme activity and diminish ROS production and oxidative damage in these embryos further supports a role of the NOX enzymes in ROS generation in ethanol-exposed GD 9 mouse embryos. DPI is a well-characterized and potent NOX inhibitor (O'Donnell et al., 1993). Because it can inhibit all NOX and DUOX isoforms at low micromolar concentrations, DPI has been widely used to provide evidence for the presence of NOX activity in tissue (Bayraktutan et al., 1998; Deme et al., 1994; O'Donnell et al., 1993; Pagano et al., 1995). However, because the mechanism of its action involves accepting an electron from flavin, DPI inhibits not only NOX enzymes, but also a number of other flavin dependent enzymes (O'Donnell et al., 1994). Nevertheless, DPI has been used extensively for validating targets for NOX-dependent pathology *in vivo*. It has been shown, in a model of hemorrhagic shock, that administration of 1mg/kg DPI resulted in a decrease in superoxide anion production, and attenuation of lung and intestinal injury (Abdelrahman et al., 2005). Treatment with 1mg/kg DPI for 4 weeks dramatically protected against alcohol-induced liver injury in the rat and diminished by 90% of free radical adducts in the bile (Kono et al., 2001). In addition, inhibition of NOX enzymes by DPI has been shown to decrease cellular ROS production (Borchi et al., 2008; Kim et al., 2008; Thakur et al., 2006), suppress p53 activation and apoptosis in a malignant skin keratinocyte cell line (Zhao et al., 2006), and decrease apoptosis in neurons (Tammariello et al., 2000). Consistent with this, we have illustrated that inhibition of NOX by DPI greatly reduces ethanol-mediated activation of caspase-3 and subsequent apoptosis in ethanol-exposed mouse embryos. The correlation between ethanol-induced apoptosis and subsequent malformation has been well established by numerous studies from our laboratory and others (Cartwright and Smith, 1995; Dunty, Jr. et al., 2001; Kotch and Sulik, 1992). It is well known that the agents (e.g. exogenous antioxidants) that can diminish ethanol-induced apoptosis can also prevent ethanol-induced malformation (Chen et al., 2001; Chen et al., 2004). Taken together, the results from this study lends further supports to the hypothesis that NOX is a key source of ROS that mediate ethanol's teratogenicity at this stage of development.

While it is recognized that many of the ROS generating pathways are not mutually exclusive and that several pathways may contribute to the ability of ethanol to induce a state of oxidative

stress in early mouse embryos, the results of this study have highlighted the importance of NOX enzymes in ethanol-induced teratogenesis. The discovery of NOX as a novel source of ROS in ethanol-exposed mouse embryos, along with the demonstration that chemically mediated inhibition of NOX diminishes ethanol-induced apoptosis (a key pathogenic endpoint) provides a novel framework for devising therapeutic interventions for FASD.

Acknowledgments

This work is supported by NIH grants AA017446 (S.-Y.C.), AA013908 (S.-Y.C.), AA11605 (K.K.S) and AA12974 from the National Institute on Alcohol Abuse and Alcoholism.

References

- Abdelrahman M, Mazzon E, Bauer M, Bauer I, Delbosc S, Cristol JP, Patel NS, Cuzzocrea S, Thiernemann C. Inhibitors of NADPH oxidase reduce the organ injury in hemorrhagic shock. *Shock* 2005;23:107–114. [PubMed: 15665724]
- Abel EL, Sokol RJ. Fetal alcohol syndrome is now leading cause of mental retardation. *Lancet* 1986;2:1222. [PubMed: 2877359]
- Adachi J, Mizoi Y, Fukunaga T, Ogawa Y, Ueno Y, Imamichi H. Degrees of Alcohol-Intoxication in 117 Hospitalized Cases. *Journal of Studies on Alcohol* 1991;52:448–453. [PubMed: 1943100]
- Babior BM. The leukocyte NADPH oxidase. *Isr Med Assoc J* 2002;4:1023–1024. [PubMed: 12489496]
- Bayraktutan U, Draper N, Lang D, Shah AM. Expression of a functional neutrophil-type NADPH oxidase in cultured rat coronary microvascular endothelial cells. *Cardiovascular Research* 1998;38:256–262. [PubMed: 9683929]
- Bedard K, Krause KH. The NOX family of ROS-generating NADPH oxidases: physiology and pathophysiology. *Physiol Rev* 2007;87:245–313. [PubMed: 17237347]
- Bonthius DJ, McKim RA, Koele L, Harb H, Kehrberg AH, Mahoney J, Karacay B, Pantazis NJ. Severe alcohol-induced neuronal deficits in the hippocampus and neocortex of neonatal mice genetically deficient for neuronal nitric oxide synthase (nNOS). *J Comp Neurol* 2006;499:290–305. [PubMed: 16977619]
- Borchi E, Parri M, Papucci L, Becatti M, Nassi N, Nassi P, Nediani C. Role of NADPH oxidase in H9c2 cardiac muscle cells exposed to simulated ischemia-reperfusion. *J Cell Mol Med*. 2008
- Brzezinski MR, Boutelet-Bochan H, Person RE, Fantel AG, Juchau MR. Catalytic activity and quantitation of cytochrome P-450 2E1 in prenatal human brain. *J Pharmacol Exp Ther* 1999;289:1648–1653. [PubMed: 10336564]
- Carpenter SP, Lasker JM, Raucy JL. Expression, induction, and catalytic activity of the ethanol-inducible cytochrome P450 (CYP2E1) in human fetal liver and hepatocytes. *Mol Pharmacol* 1996;49:260–268. [PubMed: 8632758]
- Carpenter SP, Savage DD, Schultz ED, Raucy JL. Ethanol-mediated transplacental induction of CYP2E1 in fetal rat liver. *J Pharmacol Exp Ther* 1997;282:1028–1036. [PubMed: 9262372]
- Cartwright MM, Smith SM. Increased Cell-Death and Reduced Neural Crest Cell Numbers in Ethanol-Exposed Embryos - Partial Basis for the Fetal Alcohol Syndrome Phenotype. *Alcoholism-Clinical and Experimental Research* 1995;19:378–386.
- Chen SY, Dehart DB, Sulik KK. Protection from ethanol-induced limb malformations by the superoxide dismutase/catalase mimetic, EUK-134. *FASEB J* 2004;18:1234–1236. [PubMed: 15208273]
- Chen SY, Sulik KK. Free radicals and ethanol-induced cytotoxicity in neural crest cells. *Alcohol Clin Exp Res* 1996;20:1071–1076. [PubMed: 8892529]
- Chen SY, Sulik KK. Iron-mediated free radical injury in ethanol-exposed mouse neural crest cells. *J Pharmacol Exp Ther* 2000;294:134–140. [PubMed: 10871304]
- Chen SY, Wilkemeyer MF, Sulik KK, Charness ME. Octanol antagonism of ethanol teratogenesis. *FASEB J* 2001;15:1649–1651. [PubMed: 11427515]
- Cui XL, Douglas JG. Arachidonic acid activates c-jun N-terminal kinase through NADPH oxidase in rabbit proximal tubular epithelial cells. *Proc Natl Acad Sci U S A* 1997;94:3771–3776. [PubMed: 9108053]

- Davis WL, Crawford LA, Cooper OJ, Farmer GR, Thomas D, Freeman BL. Generation of radical oxygen species by neural crest cells treated in vitro with isotretinoin and 4-oxo-isotretinoin. *J Craniofac Genet Dev Biol* 1990;10:295–310. [PubMed: 2175753]
- De A, Boyadjieva NI, Pastorcic M, Reddy BV, Sarkar DK. Cyclic AMP and ethanol interact to control apoptosis and differentiation in hypothalamic beta-endorphin neurons. *J Biol Chem* 1994;269:26697–26705. [PubMed: 7929402]
- Deme D, Doussiere J, Desandro V, Dupuy C, Pommier J, Virion A. The Ca²⁺/Nadph-Dependent H₂O₂ Generator in Thyroid Plasma-Membrane - Inhibition by Diphenyleneiodonium. *Biochemical Journal* 1994;301:75–81. [PubMed: 8037694]
- Dong J, Sulik KK, Chen SY. Nrf2-mediated transcriptional induction of antioxidant response in mouse embryos exposed to ethanol in vivo: implications for the prevention of fetal alcohol spectrum disorders. *Antioxid Redox Signal* 2008;10:2023–2033. [PubMed: 18759561]
- Dunty WC Jr, Chen SY, Zucker RM, Dehart DB, Sulik KK. Selective vulnerability of embryonic cell populations to ethanol-induced apoptosis: implications for alcohol-related birth defects and neurodevelopmental disorder. *Alcohol Clin Exp Res* 2001;25:1523–1535. [PubMed: 11696674]
- El Hassani RA, Benfares N, Caillou B, Talbot M, Sabourin JC, Belotte V, Morand S, Gnidehou S, Agnandji D, Ohayon R, Kaniewski J, Noel-Hudson MS, Bidart JM, Schlumberger M, Virion A, Dupuy C. Dual oxidase2 is expressed all along the digestive tract. *Am J Physiol Gastrointest Liver Physiol* 2005;288:G933–G942. [PubMed: 15591162]
- Fischer H, Gonzales LK, Kolla V, Schwarzer C, Miot F, Illek B, Ballard PL. Developmental regulation of DUOX1 expression and function in human fetal lung epithelial cells. *Am J Physiol Lung Cell Mol Physiol* 2007;292:L1506–L1514. [PubMed: 17337509]
- Forteza R, Salathe M, Miot F, Forteza R, Conner GE. Regulated hydrogen peroxide production by Duox in human airway epithelial cells. *Am J Respir Cell Mol Biol* 2005;32:462–469. [PubMed: 15677770]
- Gao HM, Liu B, Zhang W, Hong JS. Critical role of microglial NADPH oxidase-derived free radicals in the in vitro MPTP model of Parkinson's disease. *FASEB J* 2003;17:1954–1956. [PubMed: 12897068]
- Geiszt M, Witta J, Baffi J, Lekstrom K, Leto TL. Dual oxidases represent novel hydrogen peroxide sources supporting mucosal surface host defense. *FASEB J* 2003;17:1502–1504. [PubMed: 12824283]
- Green ML, Singh AV, Zhang YZ, Nemeth KA, Sulik KK, Knudsen TB. Reprogramming of genetic networks during initiation of the fetal alcohol syndrome. *Developmental Dynamics* 2007;236:613–631. [PubMed: 17200951]
- Halliwell B. Reactive oxygen species in living systems: source, biochemistry, and role in human disease. *Am J Med* 1991;91:14S–22S. [PubMed: 1928205]
- Hamilton ML, Van Remmen H, Drake JA, Yang H, Guo ZM, Kewitt K, Walter CA, Richardson A. Does oxidative damage to DNA increase with age? *Proc Natl Acad Sci U S A* 2001;98:10469–10474. [PubMed: 11517304]
- Harrison R. Structure and function of xanthine oxidoreductase: where are we now? *Free Radic Biol Med* 2002;33:774–797. [PubMed: 12208366]
- Heaton MB, Paiva M, Madorsky I, Siler-Marsiglio K, Shaw G. Effect of bax deletion on ethanol sensitivity in the neonatal rat cerebellum. *J Neurobiol* 2006;66:95–101. [PubMed: 16215995]
- Henderson GI, Chen JJ, Schenker S. Ethanol, oxidative stress, reactive aldehydes, and the fetus. *Front Biosci* 1999;4:D541–D550. [PubMed: 10369807]
- Infanger DW, Sharma RV, Davisson RL. NADPH oxidases of the brain: distribution, regulation, and function. *Antioxid Redox Signal* 2006;8:1583–1596. [PubMed: 16987013]
- Kim WH, Goo SY, Shin MH, Chun SJ, Lee H, Lee KH, Park SJ. *Vibrio vulnificus*-induced death of Jurkat T-cells requires activation of p38 mitogen-activated protein kinase by NADPH oxidase-derived reactive oxygen species. *Cell Immunol* 2008;253:81–91. [PubMed: 18571150]
- Kono H, Rusyn I, Uesugi T, Yamashina S, Connor HD, Dikalova A, Mason RP, Thurman RG. Diphenyleneiodonium sulfate, an NADPH oxidase inhibitor, prevents early alcohol-induced liver injury in the rat. *American Journal of Physiology-Gastrointestinal and Liver Physiology* 2001;280:G1005–G1012. [PubMed: 11292610]
- Kotch LE, Chen SY, Sulik KK. Ethanol-induced teratogenesis: free radical damage as a possible mechanism. *Teratology* 1995;52:128–136. [PubMed: 8638252]

- Kotch LE, Sulik KK. Experimental fetal alcohol syndrome: proposed pathogenic basis for a variety of associated facial and brain anomalies. *Am J Med Genet* 1992;44:168–176. [PubMed: 1456286]
- Lambeth JD. NOX enzymes and the biology of reactive oxygen. *Nat Rev Immunol* 2004;4:181–189. [PubMed: 15039755]
- Lu Y, Cederbaum AI. CYP2E1 and oxidative liver injury by alcohol. *Free Radic Biol Med* 2008;44:723–738. [PubMed: 18078827]
- Miller AA, Drummond GR, Sobey CG. Novel isoforms of NADPH-oxidase in cerebral vascular control. *Pharmacol Ther* 2006;111:928–948. [PubMed: 16616784]
- Napper RM, West JR. Permanent neuronal cell loss in the cerebellum of rats exposed to continuous low blood alcohol levels during the brain growth spurt: a stereological investigation. *J Comp Neurol* 1995;362:283–292. [PubMed: 8576439]
- O'Donnell BV, Tew DG, Jones OT, England PJ. Studies on the inhibitory mechanism of iodonium compounds with special reference to neutrophil NADPH oxidase. *Biochem J* 1993;290(Pt 1):41–49. [PubMed: 8439298]
- Odonnell VB, Smith GCM, Jones OTG. Involvement of Phenyl Radicals in Iodonium Compound Inhibition of Flavoenzymes. *Molecular Pharmacology* 1994;46:778–785. [PubMed: 7969060]
- Olney JW, Tenkova T, Dikranian K, Muglia LJ, Jermakowicz WJ, D'Sa C, Roth KA. Ethanol-induced caspase-3 activation in the in vivo developing mouse brain. *Neurobiol Dis* 2002;9:205–219. [PubMed: 11895372]
- Pagano PJ, Ito Y, Tornheim K, Gallop PM, Tauber AI, Cohen RA. An NADPH Oxidase Superoxide-Generating System in the Rabbit Aorta. *American Journal of Physiology-Heart and Circulatory Physiology* 1995;37:H2274–H2280.
- Pedrucci E, Guichard C, Ollivier V, Driss F, Fay M, Prunet C, Marie JC, Pouzet C, Samadi M, Elbim C, O'dowd Y, Bens M, Vandewalle A, Gougerot-Pocidallo MA, Lizard G, Ogier-Denis E. NAD(P)H oxidase Nox-4 mediates 7-ketocholesterol-induced endoplasmic reticulum stress and apoptosis in human aortic smooth muscle cells. *Mol Cell Biol* 2004;24:10703–10717. [PubMed: 15572675]
- Qin F, Patel R, Yan C, Liu W. NADPH oxidase is involved in angiotensin II-induced apoptosis in H9C2 cardiac muscle cells: effects of apocynin. *Free Radic Biol Med* 2006;40:236–246. [PubMed: 16413406]
- Ramachandran V, Watts LT, Maffi SK, Chen J, Schenker S, Henderson G. Ethanol-induced oxidative stress precedes mitochondrially mediated apoptotic death of cultured fetal cortical neurons. *J Neurosci Res* 2003;74:577–588. [PubMed: 14598302]
- Roebuck TM, Mattson SN, Riley EP. A review of the neuroanatomical findings in children with fetal alcohol syndrome or prenatal exposure to alcohol. *Alcohol Clin Exp Res* 1998;22:339–344. [PubMed: 9581638]
- Sulik KK, Johnston MC, Webb MA. Fetal Alcohol Syndrome - Embryogenesis in A Mouse Model. *Science* 1981;214:936–938. [PubMed: 6795717]
- Sumimoto H. Structure, regulation and evolution of Nox-family NADPH oxidases that produce reactive oxygen species. *FEBS J* 2008;275:3249–3277. [PubMed: 18513324]
- Tammariello SP, Quinn MT, Estus S. NADPH oxidase contributes directly to oxidative stress and apoptosis in nerve growth factor-deprived sympathetic neurons. *J Neurosci* 2000;20:RC53. [PubMed: 10627630]
- Thakur V, Pritchard MT, McMullen MR, Wang Q, Nagy LE. Chronic ethanol feeding increases activation of NADPH oxidase by lipopolysaccharide in rat Kupffer cells: role of increased reactive oxygen in LPS-stimulated ERK1/2 activation and TNF-alpha production. *J Leukoc Biol* 2006;79:1348–1356. [PubMed: 16554353]
- Tran TD, Jackson HD, Horn KH, Goodlett CR. Vitamin E does not protect against neonatal ethanol-induced cerebellar damage or deficits in eyeblink classical conditioning in rats. *Alcohol Clin Exp Res* 2005;29:117–129. [PubMed: 15654300]
- Webster WS, Walsh DA, McEwen SE, Lipson AH. Some teratogenic properties of ethanol and acetaldehyde in C57BL/6J mice: implications for the study of the fetal alcohol syndrome. *Teratology* 1983;27:231–243. [PubMed: 6867945]
- Wentzel P, Rydberg U, Eriksson UJ. Antioxidative treatment diminishes ethanol-induced congenital malformations in the rat. *Alcohol Clin Exp Res* 2006;30:1752–1760. [PubMed: 17010142]

Wu D, Cederbaum AI. Alcohol, oxidative stress, and free radical damage. *Alcohol Res Health* 2003;27:277–284. [PubMed: 15540798]

Zhao Y, Chaiswing L, Bakthavatchalu V, Oberley TD, St Clair DK. Ras mutation promotes p53 activation and apoptosis of skin keratinocytes. *Carcinogenesis* 2006;27:1692–1698. [PubMed: 16613839]

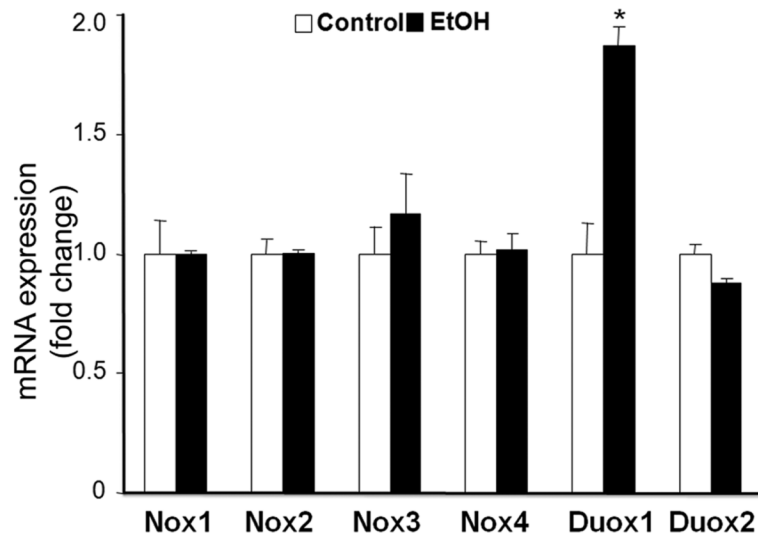


Figure 1.

Ethanol exposure results in a significant increase in mRNA expression of NOX catalytic subunit Duox1 in mouse embryos. mRNA expression of NOX catalytic subunits was determined by RT-PCR in GD 9 mouse embryos treated with Ringer's solution (Control) or 2.9 g/kg ethanol (EtOH). All data are expressed as fold change over control and represent the mean \pm SEM of three separate experiments. * $p < 0.05$ vs. control.

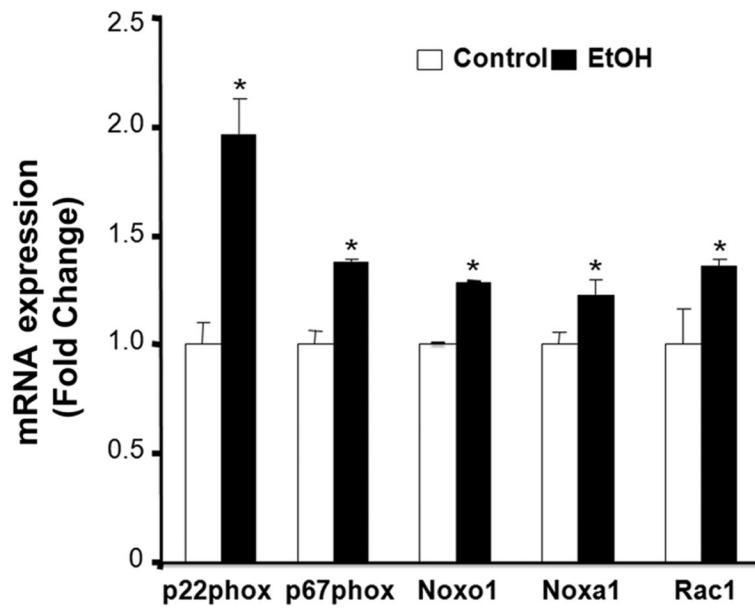


Figure 2.

Ethanol exposure significantly increases mRNA expression of NOX regulatory subunits in mouse embryos. mRNA expression of NOX regulatory subunits was determined by RT-PCR in GD 9 mouse embryos treated with Ringer's solution (Control) or 2.9 g/kg ethanol (EtOH). All data are expressed as fold change over control and represent the mean \pm SEM of three separate experiments. * $p < 0.05$ vs. control.

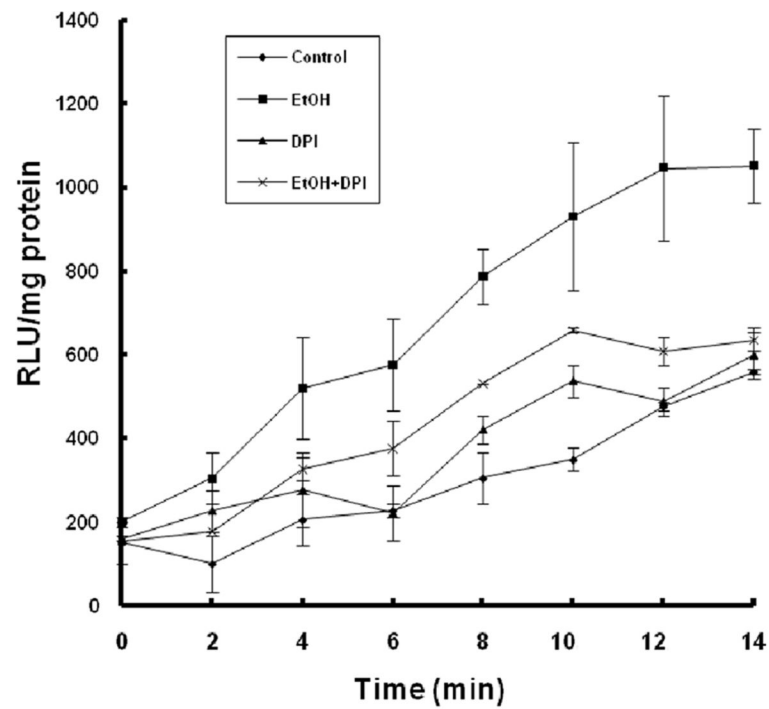


Figure 3. Co-treatment with DPI significantly prevents ethanol-induced increases in NOX activity in mouse embryos. NOX activity was measured in GD 9 mouse embryos 6 hours after exposure to Ringer's solution (Control), 2.9 g/kg ethanol (EtOH), treatment with 4 mg/kg DPI (DPI) or co-treatment with both ethanol and DPI (EtOH+DPI). Data are expressed as relative light units (RLU) and represent the mean \pm SEM of three separate experiments.

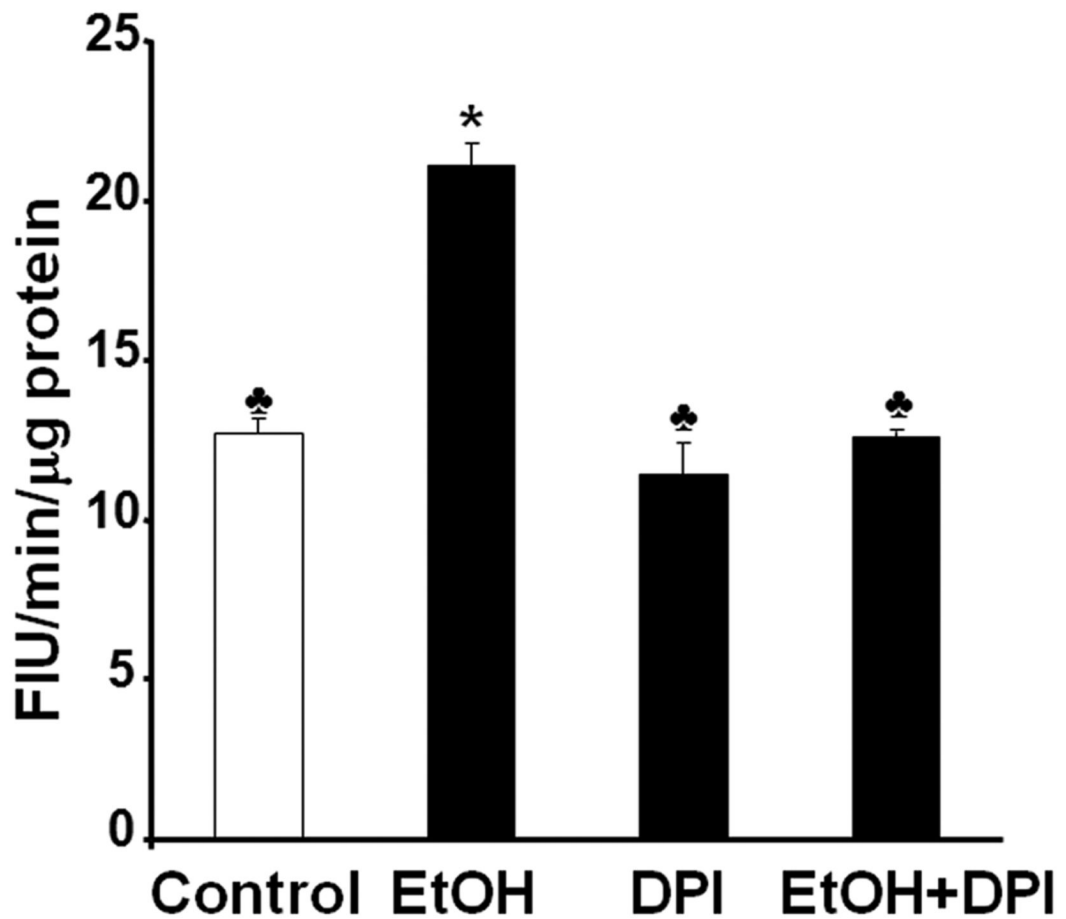


Figure 4. DPI significantly prevents ethanol-induced increase in ROS generation in mouse embryos exposed to ethanol *in vivo*. ROS generation was measured in GD 9 mouse embryos 6 hours after exposure to Ringer's solution (Control), 2.9 g/kg ethanol (EtOH), treatment with 4 mg/kg DPI alone (DPI) or treatment with both ethanol and DPI (EtOH+DPI). Data are expressed as relative fluorescence intensity units (FIU) and represent the mean \pm SEM of three separate experiments. * $p < 0.05$ vs. control. ♣ $p < 0.05$ vs. EtOH.

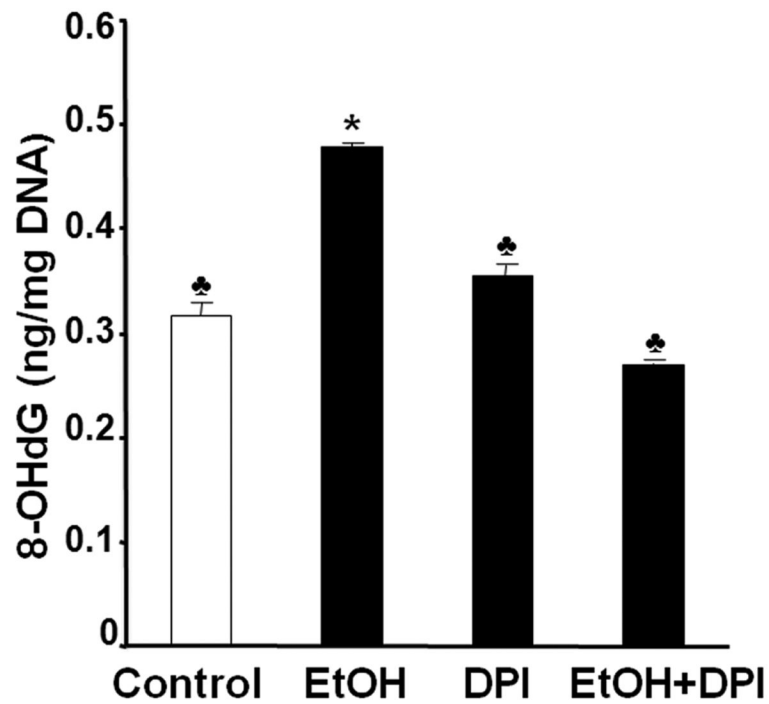


Figure 5.

Co-treatment with DPI significantly decreases oxidative DNA damage in mouse embryos exposed to ethanol *in vivo*. Level of 8-OHdG, a sensitive index of oxidative DNA damage, was determined in GD 9 mouse embryos 6 hours after exposure to Ringer's solution (Control), 2.9 g/kg ethanol (EtOH), treatment with 4 mg/kg DPI alone (DPI) or treatment with both ethanol and DPI (EtOH+DPI). Data are expressed as the mean \pm SEM of three separate experiments.

* $p < 0.05$ vs. control. ♣ $p < 0.05$ vs. EtOH.

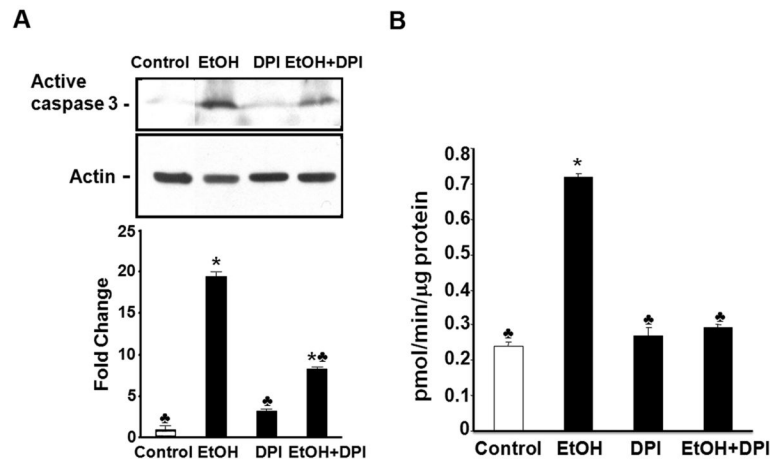


Figure 6. Co-treatment with DPI decreases the activation and activity of caspase-3 in mouse embryos exposed to ethanol *in vivo*. Western blot analyses and fluorimetric assay were performed to examine the activation (A) and activity (B) of caspase-3, respectively, in GD 9 mouse embryos 12 hours after exposure to Ringer's solution or ethanol. Embryo lysates were prepared from embryos treated with Ringer's solution (Control), 2.9 g/kg ethanol (EtOH), treated with 4 mg/kg DPI alone (DPI) or treated with both ethanol and DPI (EtOH+DPI). Data are expressed as fold change over control and represent the mean \pm SEM of three separate experiments. * $p < 0.05$ vs. control. ♣ $p < 0.05$ vs. EtOH.

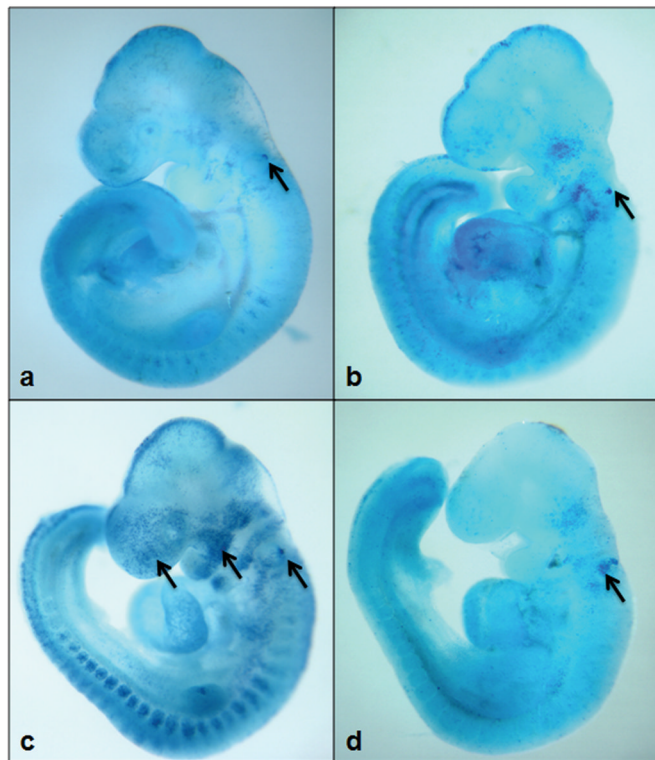


Figure 7. DPI treatment reduces ethanol-induced apoptosis. Nile blue sulfate vital staining of comparably staged mouse embryos treated with Ringer's solution (Control) (a), DPI (b), 2.9 g/kg ethanol (c), or treated with both ethanol and DPI (d) illustrates excessive stain uptake in mouse embryos exposed to ethanol alone (arrows are directed toward sites of specific uptake in the brain and facial region of GD 9 embryos). Co-treatment with DPI results in diminished staining in ethanol-exposed mouse embryos. Shown are representatives of 10-15 embryos from several different litters of each group.

Table 1
Sequences of primers used for quantitative real-time PCR analysis of gene expression in mouse embryos

Gene	Access. No.	Position	Forward(5'-3')	Reverse(5'-3')
NOX1	NM_172203	878F-947R	AGGTCGTGATTACCAAGGTTGTC	AAGCCTCGCTTCCTCATCTG
NOX2	NM_007807	1216F-1303R	AGCTATGAGGTGGTGATGTTAGTGG	CACAATATTTGTACCAGACAGACTTGAG
NOX3	AY573240	414F-479R	GCTGGCTGCACTTCCAAC	AAGGTGCGGACTGGATTGAG
NOX4	NM_015760	872F-983R	CCCAAGTTCCAAGCTCATTTCC	TGGTGACAGGTTTGTGCTCCT
DUOX1	XM_130483	4679F-4777R	CCACCATGCTGTACATCTGTGA	AGGGAGGGCGACCAAAGT
DUOX2	XM_619807	699F-760R	TCCAGAAGGCGCTGAACAG	GCGACCAAAGTGGGTGATG
p22	NM_007806	139F-203R	CGTGGCTACTGTGGACGTT	GCACACCTGCAGCGATAGAG
p67	BC076609	1991F-2161R	TGGACTTCGGATTACCCCTCAGTC	CACCTTGAGCATGTAAGGCATAGG
Noxa1	BC047532	343F-410R	ACTCTGCGCTGTGCTTCTTCT	ACAGCCCCTGTTAAAGTACATCCT
Noxo1	NM_027988	557F-637R	GGCAGCCTTGACATTCATAGC	TCTGTCTTTATGTCAAGAGTGTGGAA
Rac1	NM_009007	296F-364R	CCCCACCGTCTTTGACAAC	CATAGGCCAGATTCCTGGTT
GAPDH	BC023196	165F-355R	AACGACCCTTCATTGAC	TCCACGACATACTCAGCAC